SUPERCONDUCTING CRITICAL TEMPERATURE REENTRANCE IN F/S/F THREE-LAYERED STRUCTURES BASED ON Nb AND $Cu_{41}Ni_{59}$ ALLOY

Zdravkov V.I.[1,3], Obermeier G.[3], Garcia-Garcia J. [3], Kehrle J. [3], Ullrich A. [3], Müller C.[3], Morari R. [1, 2], Antropov E. [1], Horn S.[3], Tagirov L.R. [3, 4], Tidecks R.[3], Sidorenko A.S.[1, 2]
[1] D. Ghitu IIEN, ASM, Republic of Moldova
[2] Karlsrue Institute of Technology, Germany
[3] University of Augsburg, Germany
[4] Solid State Physics Department, Kazan State University, Russia

Abstract. *Ferromagnet/Superconductor/Ferromagnet (F/S/F) trilayers, in which the establishing of a Fulde-Ferrell Larkin-Ovchinnikov (FFLO) like state leads re-entrance behavior of superconductivity, form the core structure of the superconducting spin valve. The appiarance of pronounced critical temperature oscillations in such trilayers as a function of the ferromagnetic layer thicknesses and the reentrant superconductivity, are the key condition to obtain a large spin valve effect, i.e. a large shift in the critical temperature. Both phenomena have been realized experimentally in the $Cu_{41}Ni_{59}$/Nb/$Cu_{41}Ni_{59}$ trilayers, the results of investigation are presented.*

Key-words: *spintronics, thin film, F/S/F structures, re-entrant superconducting behavior, magnetron sputtering.*

I. Introduction

Superconducting layered structures based on thin films are the object for intense investigations for recent decades as a base element for superconducting electronics [1]. The investigations of proximity effect at Superconductor/Normal metal (S/N) and Superconductor/Ferromagnet (S/F) interfaces motivated the development of the advanced technologies yields high quality superconducting films with constant thicknesses and enhanced superconducting properties. Niobium is the traditional material for superconducting electronics. Unfortunately, Nb is a high chemical active metal whereas adsorbed gases which intensively affects the superconducting properties especially at the nanoscale thicknesses. On the other hand, S/F superconducting structures with Nb layers of this range of thicknesses demonstrate main interesting physical phenomena based on space oscillation of order parameter due to proximity effect [2, 3, 4], that can be the basis for elaboration super-rapid operating spin-switch [5].

Superconducting spin-switch based on proximity effect in Ferromagnet – Superconductor – Ferromagnet layered system consisting (F/S/F) of three layers was presented theoretically in [5] using hypothetical materials and their thicknesses.

Two ferromagnetic layers offer a control of the superconducting state in the S layer sandwiched between two ferromagnetic layers, if one allows for the rotation of the magnetization of one of the layers with respect to another. For a thin S layer, with a thickness d_S comparable to the superconducting coherence length ξ_S, superconductivity can be switched on and off by rotating the magnetization of one of the magnetic layers in a F/S/F trilayer [5]. In the superconducting F/S/F spin switch, the critical temperature T_c, depends on the relative direction of the magnetizations of the F layers. The T_c is lower in the parallel case compared to the antiparallel case.

Several experimental attempts [5, 6, 7, 8, 9] demonstrated existence of the spin – switch effect with maximum shift for superconducting critical temperature for parallel P and anti-parallel AP alignment of magnetizations of the ferromagnetic layers, $\Delta T_c \approx 41$ mK, but the value should be

essentially increased for real applications. One of the main problem which should be resolved for achievement of this goal is the development of the advanced vacuum technology for preparation of a high quality F/S/F samples and to find the properly range of the thicknesses of the layers, as we will demonstrate.

II. Thin Film Deposition and Sample Configuration

The spin valve core can be regarded as a F/S-S/F structure, as already discussed in [10]. Applying our wedge technique, described in detail in Refs. [3, 11], we fabricated two types of sample series (Fig. 1). In the first one, (a "single wedge" geometry, see Fig. 1a)) the bottom F-layer (made of $Cu_{41}Ni_{59}$ grown on the Si buffer layer) has a constant thickness as well as the subsequently grown 2S-layer (made of Nb). The F-layer on top (made of $Cu_{41}Ni_{59}$) has a wedge like shape. The second type (a "double wedge" geometry, see Fig. 1b)) of sample series consists of two $Cu_{41}Ni_{59}$ wedges separated by a Nb layer of constant thickness. We used a ($80\times7mm^2$ size) commercial (111) Si substrate on which a sample series was magnetron sputtered at the same run. To get a series of 30-35 separate samples cuts of equal distance (about 2.5 mm) were made, following the long side of the substrate, perpendicular to the wedge.

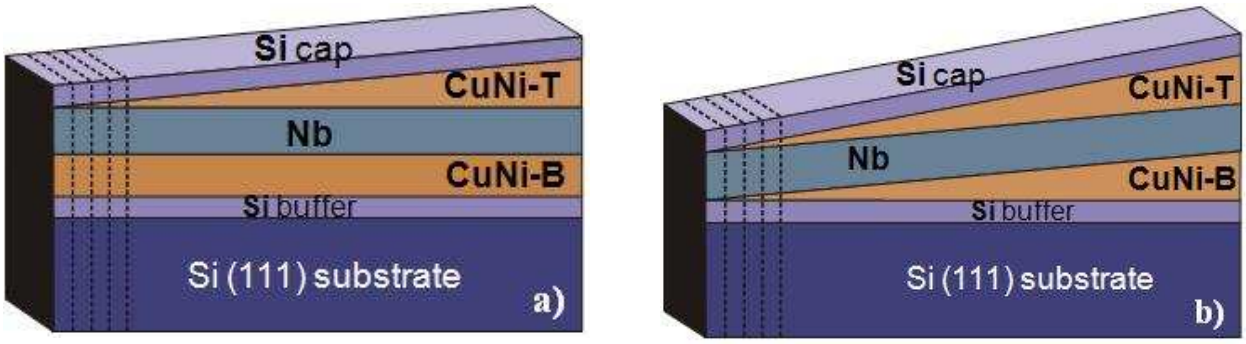

Fig. 1: Wedge technique to fabricate $Cu_{41}Ni_{59}$/Nb/ $Cu_{41}Ni_{59}$ trilayers. a) Single wedge geometry: Bottom $Cu_{41}Ni_{59}$ layer ("CuNi-B") kept at a constant thickness. Top $Cu_{41}Ni_{59}$ layer ("CuNi-T") wedge-type. b) Double wedge geometry: Both $Cu_{41}Ni_{59}$ layers are wedges. The symmetric situation is drawn, where the slope of both wedges is the same. In both geometries the thickness of the Nb layer is constant.

III. Samples Analysis

Thickness Analysis

Rutherford Backscattering Spectrometry (RBS) was applied to determine the thickness of the individual layers. In Fig. 2a the results of an RBS evaluation are shown for the single wedge geometry (sample series FSF1). The thickness of the layers (CuNi-Top, CuNi-Bottom and Nb) has been plotted as a function of the sample number, i.e. the distance from the thick end of the $Cu_{41}Ni_{59}$ alloy wedge. The bottom CuNi alloy film as well as the Nb film have nearly constant thickness. In Fig. 2b) a similar representation is shown for the double wedge geometry. Again, the Nb film has a constant thickness, whereas the thickness of the CuNi alloy wedges change continuously along the sample series. It is remarkable that for a given sample the thickness of both CuNi alloy films is always nearly equal.

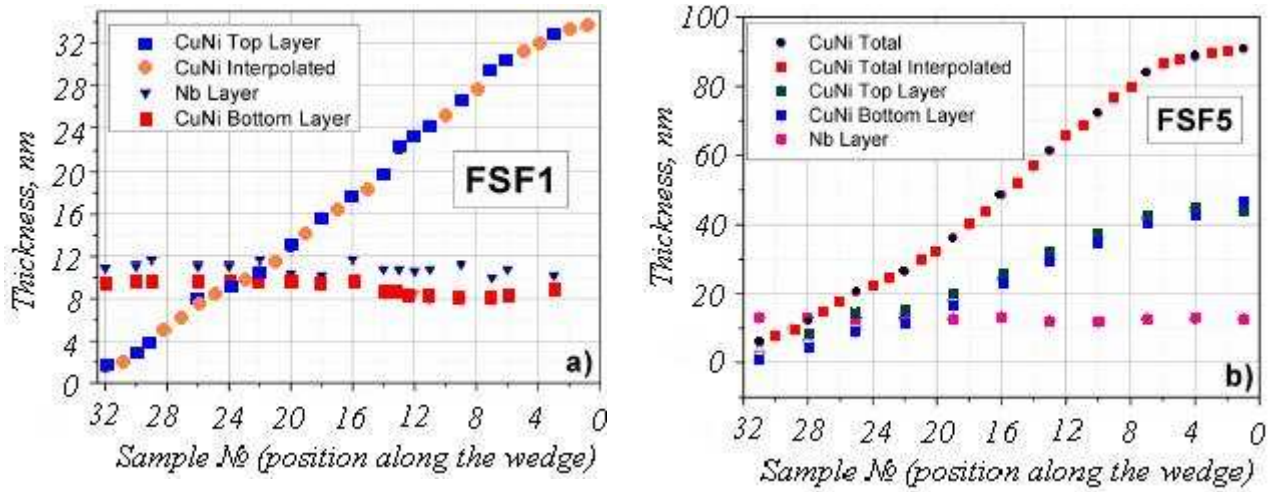

Fig. 2: Results of RBS measurements for the thickness of the respective films in F/S/F ($Cu_{41}Ni_{59}$/Nb/ $Cu_{41}Ni_{59}$) trilayers plotted against the sample number starting at the thick end of the wedge. a) Single wedge sample series FSF1. Some of the data points of the $Cu_{41}Ni_{59}$ Top layer are interpolated values between two RBS measurements b) Double wedge sample series FSF5. Some of the data points of the sum of the thicknesses of both $Cu_{41}Ni_{59}$ layers ("CuNi Total") are interpolated values between two RBS measurements.

Transmission Electron Microscopy

The growth of our $Cu_{1-x}Ni_x$/Nb/$Cu_{1-x}Ni_x$ samples has been studied by cross sectional Transmission Electron Microscopy (TEM) using a JEOL JEM 2100F microscope with a GATAN imaging filter and CCD camera. In Fig. 3a) an overview of sample No5 of the Si(substrate)/Si(buffer)/$Cu_{1-x}Ni_x$/Nb/ $Cu_{1-x}Ni_x$ /Si(cap) single wedge geometry of the FSF1 series is shown.

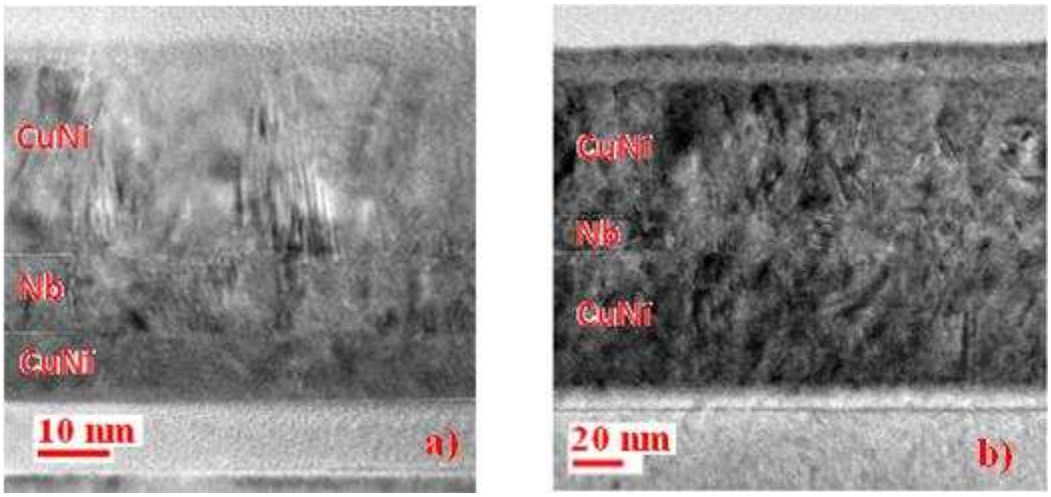

Fig 3: Transmission Electron Microscopy images: a) Overview over the cross section of specimen No5, taken from the single-wedge FSF1 sample; b) Overview over the cross section of specimen No2, taken from the double wedge sample FSF5.

The overview over the cross sections of sample FSF1 No5 and FSF5 No2, respectively, show straight and clearly defined boundaries between the different materials over an extended area.

For this sample the interpolated thicknesses (specimen not subjected to the RBS procedure before investigated) from Fig. 2a) are 8.6 nm, 10.6 nm, and 31.2 nm for the bottom $Cu_{41}Ni_{59}$ layer,

the Nb layer and the top $Cu_{41}Ni_{59}$ alloy layer, respectively. In Fig. 3b) sample No2 of the double wedge geometry series FSF5 is shown. In this case we have from Fig. 2b) the thicknesses 44.6 nm, 12.7 nm, and 45.5 nm from interpolated RBS data. Both layer thicknesses are in agreement with the TEM picture within about 10%.

IV. Superconducting Properties

The transition temperature of the trilayers was obtained as the midpoint of their resistance-temperature transition curves measured in a Helium-3 cryostat and a dilution refrigerator. The standard dc four probe techniques (10μA measuring current for 0.4-10K and 2μA for 40mK-1K) was applied. To eliminate thermoelectric voltages, alternating the polarity of the current during measurement was done.

In Fig. 4a) the resulting transition temperature for the single wedge series is shown as a function of the thickness of the top F-layer, which changes along the sample series. The average thickness of the constant bottom layer is given in addition. For sample series FSF1 and FSF2 the thickness of the bottom $Cu_{41}Ni_{59}$ alloy film is in average 9.0 nm (see Fig. 2a) and 6.2 nm, respectively. In case of the double wedge samples FSF3 and FSF5 shown in Fig. 4b), the sum of the thicknesses of both F-layers is used. For the FSF5 series the thickness of both layers is nearly the same as seen from the RBS data given in Fig. 2. For the sample series FSF3 the thickness of the top layer increases somewhat more strongly along the wedge compared to the thickness of the bottom layer. For sample #1 and #19 of the upper wedge with dCuNi-T=47.4nm and 14.7 nm the difference to the lower wedge with the smaller thickness is 7.9 nm and 2.3 nm, respectively. Between these samples both thicknesses show nearly a straight line behavior as a function of the sample number.

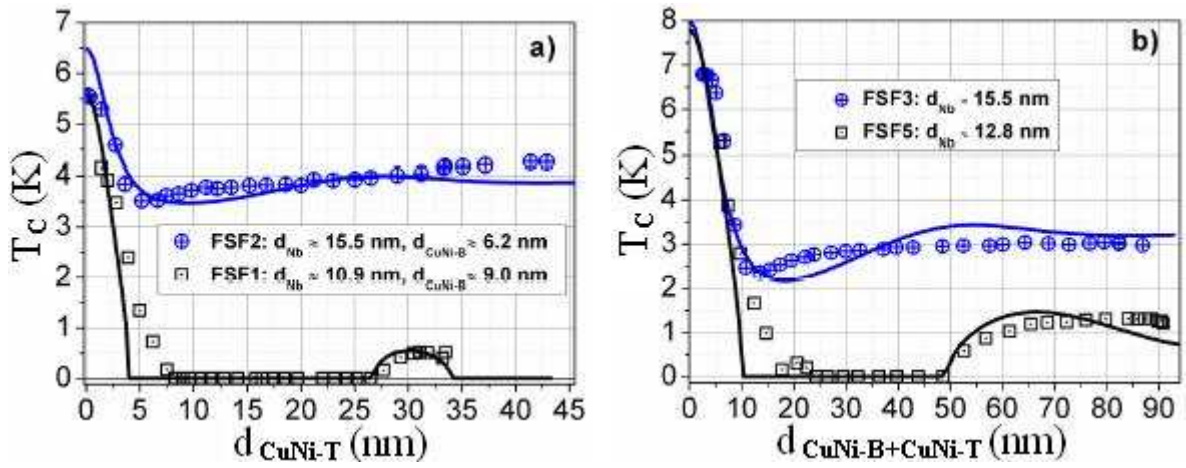

Fig. 4: Transition temperatures, T_c, of the investigated $Cu_{41}Ni_{59}$ /Nb/ $Cu_{41}Ni_{59}$ trilayer samples as a function of the thickness *d*CuNi of the $Cu_{41}Ni_{59}$ alloy layers. a) Single wedge sample series FSF1 and FSF2. Critical temperature as a function of the increasing thickness of the top layer *d*CuNi-T. Thickness *d*CuNi-B of the bottom flat $Cu_{41}Ni_{59}$ layer and the niobium layer is given in the figure. b) Double wedge series FSF3 and FSF5 plotted as a function of the sum of the thickness of the bottom and top layer, *d*CuNi-B+*d*CuNi-T. The thickness of the niobium layer is given in the figure.

For both types of sample series for a larger thickness of the S-layer an oscillation of the critical temperature is observed. Reducing the thickness of the Nb layer, then yields a reentrant superconducting behaviour.

V. Conclusion

The non-monotonous behavior of the critical temperature of $Cu_{41}Ni_{59}/Nb/Cu_{41}Ni_{59}$ trilayers is investigated as a function of the thickness of the ferromagnetic layers. Oscillations of the critical temperature and the reentrant behavior of the superconducting state could be realized in two different types of sample geometries. In the first one, the symmetric case, the thickness of the ferromagnetic material of both layers changes equally while the thickness of the superconducting material is held constant. In the second type, the asymmetric case, the thickness of one of the ferromagnetic layers is constant while the thickness of the second layer was varied, keeping the constant thickness of the superconducting material.

These experiments represent an important step towards the superconducting spin valve construction, which needs a Ferromagnet/Superconductor/Ferromagnet core structure with an oscillatory or, more optimal, a reentrant superconducting behavior to realize the theoretically predicted spin switch effect.

VI. Acknowledgments

The work was supported by DFG grant AOBJ: 573661, by the A.v.Humboldt Foundation AvH grant "Nonuniform superconductivity in layered SF-nanostructures Superconductor/Ferromagnet", and Moldavian State Program Grant 11.836.05.01A.

VII. References

1. Buzdine A.I. Proximity effects in superconductor-ferromagnet heterostructures. Rev. Mod. Phys. 2005, vol. 77, pp. 935–976 ;
2. Tagirov L.R. Proximity effect and superconducting transition temperature in superconductor/ferromagnet sandwiches, Physica C, 1998, vol. 307, N1-2, pp. 145-163
3. Zdravkov, V.; Sidorenko, A., Obermeier, G., Gsell, S.; Schreck, M.; Müller, C.; Horn, S.; Tidecks, R.; Tagirov, L.R. Re-entrant superconductivity in Nb/Cu_xNi_{1-x} bilayers. Phys. Rev. Let., 2006, v. 97, pp. 057004 (1-4);
4. Ryazanov V. V., Obozhov V. A., Rusanov A. Yu., Veretennikov V. A., Golubov A. A., Aarts J., Phys. Rev. Lett. 2001, vol. 86, p. 2427;
5. Tagirov L.R. Low-field superconducting spin switch based on a superconductor/ferromagnet multilayer, Phys. Rev. Lett., 1999, v.83, N10, p.2058-2061;
6. Ogrin F. Y. ,Lee S. L., Hillier A. D., Mitchell A., and ShenT.-H., Phys. Rev. B 2000, vol. **62**, pp. 6021- 6026;
7. Schöck M., Sürgers C., and Löhneysen H. v., Eur. Phys. J. B 2000, vol. **14**, pp. 1-14.
8. Kim J., Kwon J. H., Char K., Doh H., Choi H. Y., Phys. Rev. B 2005, vol. **72**, pp. 014518.
9. Sidorenko A. et al. Journal of Physics: Conference Series**,** 2009, vol. 150, pp. 052242 (1-4)
10. Zdravkov V. I., Kehrle J., Obermeier, Ullrich A., Gsell S., Lenk D., Müller C., Morari R., Sidorenko A. S., Ryazanov V. V., Tagirov L., Tidecks R., and Horn S.. Interference Effects of the superconducting Pairing Wave Function due to the Fulde-Ferrell-Larkin-Ovchinnikov like State in Ferromagnet/Superconductor Bilayers. Supercond. Sci. Technol., 2011, vol. 24, p. 095004 (1-7)
11. Zdravkov V. I., Kehrle J., Obermeier G., Gsell S., Schreck M., Müller C., Krug H.-A. von Nidda, Lindner J., Moosburger J.-Will, Nold E., Morari R., Ryazanov V. V., Sidorenko A. S., Horn S., Tidecks R., and Tagirov L. R. Reentrant superconductivity in superconductor/ferromagnetic-alloy bilayers. Phys. Rev. B 2010, vol. 82, p. 054517(1-13)